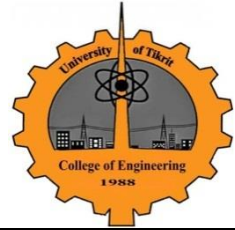


TJES

ISSN: 1813-162X

Tikrit Journal of Engineering Sciences

available online at: <http://www.tj-es.com>



Mechanical and Physical Properties of Hybrid Cu-Graphite Composites Prepared via Powder Metallurgy Technique

Farouk M. Mahdi^{1*}, Jawadat A. Eaqoob², Fouad R. Muhialdeen³

¹Mechanical Engineering Department, Tikrit University, Salahaldeen, Iraq

E-Mail: Farouk_engineering@yahoo.com

² Technical College, Kirkuk, Iraq

³ Mechanical Engineering Department, Tikrit University, Salahaldeen, Iraq

(Received 11 May 2016, Accepted 28 July 2016, Available online 31 March 2017)

Abstract

Copper-graphite composites are widely used in a great number of engineering applications such as brushes, switches, sliding bearings, self-lubricating bearings, etc. due to their good thermal and electrical conductivity and excellent tribological properties as compared with other structural materials. There are ongoing attempts in manufacturing copper composites with better properties to enhance their efficiency and increase their effective life. Present research aims to prepare hybrid 95wt.% copper –5wt.% graphite composites reinforced with yttria and tin particles by powder metallurgy technique and to study their effects on mechanical and physical properties of the prepared composites. Powder mixture was mixed by ball mill mixer at 100rpm for 120min with (5/1) balls to powder ratio. The powder mixture was cold pressed at 700MPa for 30sec, followed by sintering at 900 °C for one hour. In the first stage, Yttria(Y₂O₃) was added with (2, 4, 6, 8, 10) wt% to pure copper (Cu) and to (95%Cu-5%Gr) matrices. Typical composite of this stage was ((95%Cu-5%Gr)-4%Y₂O₃). In the second stage, tin (Sn) was added with (2, 4, 6, 8, 10) wt% to pure copper and((95%Cu-5%Gr)-4%Y₂O₃ matrices. Typical composite of this stage was ((95%Cu-5%Gr)-4%Y₂O₃)-6%Sn. The results showed that hardness and true porosity of the composites increases with increasing yttria content. On the other hand, both thermal and electrical conductivity of the composites decreases with increasing yttria content. It was also found that (95 wt.% Cu- 5 wt.% Gr) – Y₂O₃ composites have always lower wear rate than plain Cu-Y₂O₃ composites.

Keywords: Hybrid Copper-Graphite Composites, powder metallurgy.

الخواص الميكانيكية والفيزيائية لمتراكبات هجينة ذات اساس من النحاس- الكرافيت محضرة بطريقة ميتالورجيا المساحيق

الخلاصة

تستخدم متراكبات النحاس- الكرافيت على نطاق واسع في عدد كبير من التطبيقات الهندسية مثل الفرش الكهربائية، والمفاتيح، والمحامل الانزلاقية، ومحامل التزيت الذاتي وغيرها بسبب امتلاكها الموصلية الحرارية والكهربائية الجيدة والخواص الترابولوجية الممتازة بالمقارنة مع المواد التركيبية الأخرى. هناك محاولات مستمرة في تصنيع مركبات النحاس ذات خواص أفضل لتحسين كفاءتها وزيادة عمرها بشكل مؤثر. يهدف البحث الحالي إلى تحضير متراكبات هجينة ذات أرضية من النحاس 95% والكرافيت 5% بتقانة ميتالورجيا المساحيق ودراسة تأثير المضافات على الخواص الميكانيكية

والفيزيائية للمتراكبات المحضرة. تم خلط المساحيق بواسطة خلاط (طاحونة كروية) لمدة 120 دقيقة وبسرعة 100 دورة/دقيقة ونسبة الكرات الى المساحيق (1/5). تم كبس خليط المساحيق تحت ضغط 700 ميكاباسكال لمدة 30 ثانية واتبعت بالتليد عند 900 درجة مئوية لمدة ساعة واحدة. اضيفت البتريا بنسب وزنية (2، 4، 6، 8، 10) الى ارضية النحاس النقي والى المتراكب المثالي في هذه المرحلة (95%Cu-5%Gr). المتراكب المثالي الناتج من هذه المرحلة هو ((95%Cu-5%Gr-4%Y₂O₃)). في المرحلة الثانية، اضيفت القصدير بنسب وزنية (2، 4، 6، 8، 10) الى ارضية النحاس النقي والى ارضية ((95%Cu-5%Gr-4%Y₂O₃)). إن المتراكب المثالي في هذه المرحلة هو ((95%Cu-5%Gr-4%Y₂O₃)-6%Sn). اظهرت النتائج زيادة في الصلادة والمسامية الحقيقية مع زيادة محتوى البتريا. هذا من جهة ومن جهة اخرى تقل كل من التوصيلية الحرارية والكهربائية مع زيادة محتوى البتريا. وجد كذلك أن معدل البلى لمتراكبات Cu-Y₂O₃ - Y₂O₃ (95 wt.% Cu- 5 wt.% Gr) يكون دائماً أقل من معدل البلى لمتراكبات Cu-Y₂O₃

الكلمات الدالة: متراكبات نحاس – كرافيت الهجينة، ميتالورجيا المساحيق

Introduction

In the last few years, several attempts have been done to reinforce copper in order to improve its mechanical properties. Copper is one of the most promising metals because of its high electrical and thermal conductivity, superior corrosion and oxidation resistance. However due to its relatively high ductility, low yield strength, weak creep resistance and low hardness, it is necessary when increasing its mechanical properties be careful not to greatly affect its electrical properties[1]. Structural materials composed of matrix material and reinforcement material are called composite materials which combine the properties of two or more components [2, 3]. Using single reinforcement in copper matrix may sometimes lead to the deterioration of its physical and mechanical properties. To overcome these losses in copper properties, hybrid composites are prepared from two or more different types of reinforcements with copper matrix. Oxides of metals like aluminum, cerium, yttrium and zirconium are often used for this purpose as fine and uniformly distributed dispersoid particles in soft and ductile copper matrix. Such composites find applications as electrical contacts, resistance-welding tips, lead wires, continuous casting molds, etc.[4]. The most common routes for particle-reinforced Cu matrix composites include casting and powder metallurgy methods. Powder metallurgy (PM) is preferred to casting because of low agglomeration, low segregation and good wettability[5, 6].

PM processing includes mixing, pressing and sintering[7]. Graphite plays a significant role in advanced energy materials with excellent tribological properties [8]. Copper-graphite composites, produced by powder metallurgy processes

are now widely used in tribological engineering parts, such as bearings, and electrical contact parts, notably carbon brushes for engines and generators[9]. Dongdong Gu and Yifu Shen[10] found that mixing variables and powder characteristics such as particle shape and particle size distribution have great effects on sintered density and microstructural homogeneity of Cu-(Sn,Pb) composites. Montasser Dewidar et.al.[11] studied the effect of processing parameters and amount of additives on the mechanical properties and wear resistance of copper-based composite. They found that increasing the graphite content up to 5 wt% increase the wear resistance of the Cu-(Sn, Pb) composites. Yongping Jin and Ming Hu[12] achieved near full densification in copper – graphite composite through pressing at 700 MPa for 30 sec, followed by sintering at 900 °C for 1 hr. Chandana Priyadarshini Samal[13] studied the effect of process parameters on the hardness and microstructure of copper – graphite composites prepared by powder metallurgy route. He found that the optimum compacting pressure, sintering temperature and sintering time for conventional sintering were 700 MPa, 900 °C and 1 hr. respectively. Jirapat Prapai et.al.[14] studied the tribological properties of Cu matrix composites reinforced with Fe, Gr, Sn, ZrO₂ and SiO₂) prepared by PM that is used in dry friction clutch. They found that improper material formulations caused inferior properties particularly with high sintering temperatures. High Sn contents caused swelling of the sintered materials as well as tribological properties (coefficient of friction and wear resistance). It was found that the investigated materials were insensitive to sintering temperatures in the range (800-900) °C but they were strongly influenced by chemical compositions.

Experimental Procedure

Used Materials

Electrolytic copper powder ($\leq 63\mu\text{m}$ in size with 99.7% purity), graphite powder ($\leq 53\mu\text{m}$ in size with 99.9% purity), yttria powder ((10-5) μm in Size with 99.95% purity) and tin powder ($\leq 53\mu\text{m}$ in size with 99.95% purity) were selected as metal matrix, soft reinforcement, hard reinforcement and modifier respectively.

Composite Preparation

Graphite powder was preheated up to 200 °C for two hours to get rid of moisture and other volatile substances. Hybrid 95% copper–5% graphite composite is fabricated by powder metallurgy technique and prepared through two stages as illustrated in Figures 1 and 2 which represent the flow charts of the experimental procedure in stage 1 and 2 respectively.

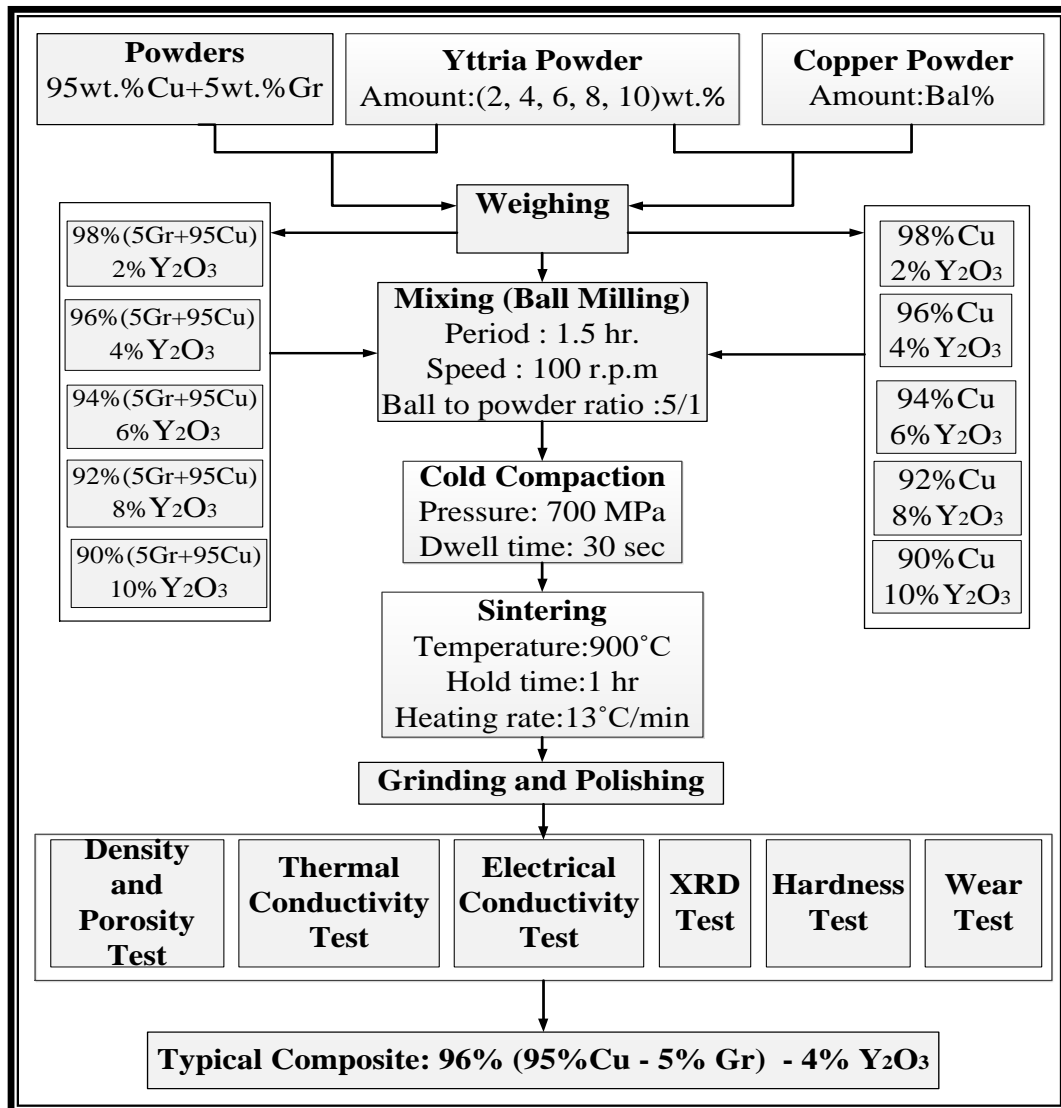


Fig. 1. Flow chart for the experimental procedure of stage-1

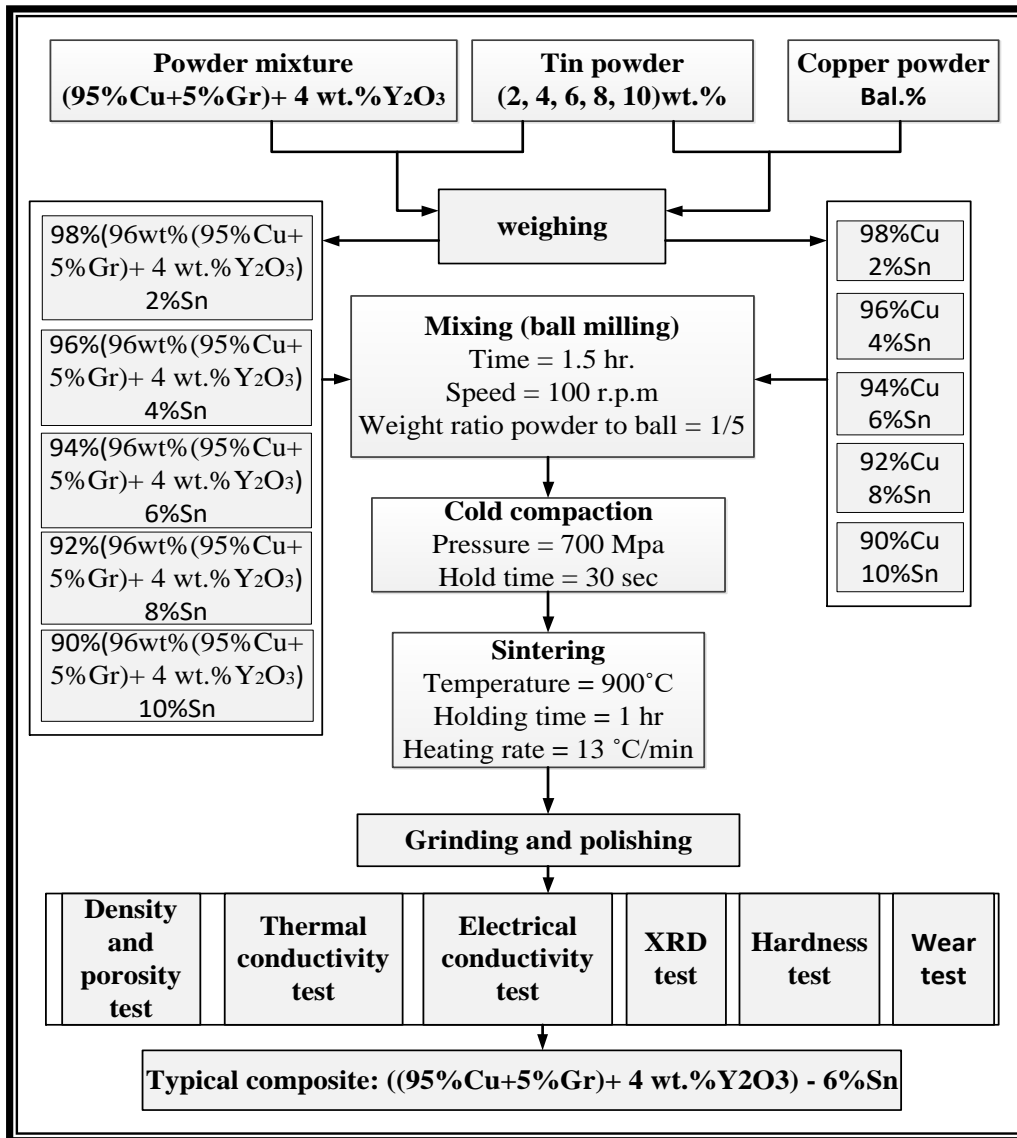


Fig. 2 .Flow chart for the experimental procedure of stage-2

The powders were mixed by mixing machine (ball milling) as shown in Figure (3) for 1.5hrs at 100rpm. 8mm diameter balls were used with 5/1 balls to powder ratio. The powder mixtures were cold pressed by uniaxial pressing at 700MPa for 30sec inside a cylindrical hardened steel die using compaction machine (type: U test, turkey) with capacity 250KN to produce green compacts with 10 mm in diameter and 7 ± 1 mm in height. The inner surface of the die was lined with thin layer of graphite to avoid the adhesion between die and

punch as well as to provide lubrication during ejection of the compact.

Green compacts were sintered at 900°C for 1hr. with heating rate 13°C/min, followed by cooling inside an electric muffle furnace. To prevent oxidation, the samples were placed in a ceramic container with multilayer graphite powder and gray cast iron chips and are sealed with castable (Alumina + silica) layer and castable magnesium oxide layer as shown in Figure (4). This configuration was proved to be effective in oxidation prevention[15]. K-type thermocable was used to measure and to

control sintering temperature inside the container.

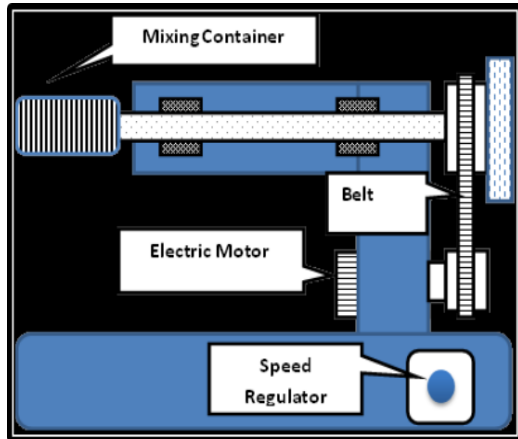


Fig. 3. Sketch for mixing machine

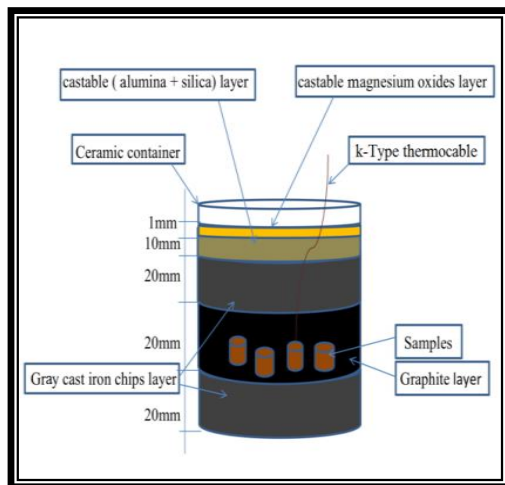


Fig. 4. Sintering container

Performance Testing

Hardness Test

The hardness of the sintered compacts was measured using Brinell hardness tester (type: Innovatest, Netherland) at a load of 30kg and a dwell time of 20sec using indentation ball of 1mm diameter. Each hardness value represents an average of ten readings.

Wear Test

Wear test was performed using a pin on disc-tribometer (P.A. Hilton Ltd Company, UK). Sintered compacts represent the pins while hardened steel disc of 218 HB was used as counter disc. Before loading the specimens on the test device, the surface of the hardened steel disc was thoroughly

cleaned with acetone. Wear tests were carried out under dry sliding condition and a normal load of 40N. The rotating speed of the steel disc was 350rpm for 30min. All experiments were carried out in ambient temperature and relative humidity of 36%. Each specimen was weighed before and after every wear test in an electronic balance with 0.1mg precision to obtain the weight loss. The wear rate was calculated according to the following formula[16]:

$$\text{Wear rate} = \frac{\Delta W}{S} \text{ (g/cm)} \dots \dots \dots (1)$$

$$\Delta W = W_1 - W_2$$

$$S = 2\pi rnt$$

W_1 = weight of specimen before the test (g)

W_2 = weight of specimen after the test (g)

S = sliding distance (cm)

r = sliding radius (cm) (from center of the disc to center of the specimen)

n = sliding speed (r.p.m)

t = sliding period (min)

Determination of Relative Density and True Porosity

Sintered or true density of the specimens was determined by Archimedes' principle according to [17]. The procedures were carried out as follows:

- 1- The test specimens were dried at 150°C for 1hr then cooled slowly to room temperature inside the oven. The dry weight of the cooled specimens (W_d) were measured.
- 2- The suspended weight (W_i) was determined by suspending and sinking the specimen inside flask containing distilled water.
- 3- The specimens were immersed in boiled distilled water for 5hrs. then followed by soaking in distilled water for an additional 24hrs. at room temperature. Subsequently, specimens were weighed after removing all excess surface water by a moistened, lint-free linen or cotton cloth to obtain weight (W_s). Relative density and porosity were determined by the following relationships [18, 19, 20]:

$$T.D = \sum_{i=1}^n (\rho_i \cdot x_i) \dots \dots \dots (2)$$

T.D = Theoretical density (g/cm³)

ρ_i = Density of element in the composite (g/cm³)

x_i = Percentage of element in the composite

$$B.D. = \frac{W_d}{W_s - W_i} \times \rho_w \dots \dots \dots (3)$$

B.D. = Bulk density (g/cm³)

W_d = Dry weight (g)

W_i = Suspended weight (g)

W_s = Saturated weight (g)

ρ_w = Water density = 1 g/cm³

$$R.D. = \frac{B.D.}{T.D.} \times 100\% \dots \dots \dots (4)$$

R.D = Relative density

$$T.P. = \frac{T.D. - B.D.}{T.D.} \times 100\% \dots \dots \dots (5)$$

T.P. = True porosity

Thermal and Electrical conductivity Test

Thermal conductivity was determined by using thermal conductivity measurement system (TechQuipment Ltd, UK). The sample was put in the device between two brass blocks; the first block was heated while the second block was cooled by current water. Electric power was applied to supply the required heat energy to heat the sample while a set of thermocouples were used to measure the temperature gradient along the two brass blocks and the supported sample between them. Heating was continued until a steady state condition between the two samples ends (ΔT) was satisfied. Fourier law was applied to calculate the thermal conductivity [20].

$$-K = \frac{Q}{A \times \frac{\Delta T}{\Delta x}} \dots \dots \dots (6)$$

Where

Q = amount of heat (W) = 10 Watt

K = thermal conductivity (W/ (m.k))

ΔT = temperature difference between the two ends of the specimen (m)

Δx = distance between the two thermocouples that measures two points on the sample (m)

A = cross section area of the specimen (m²)

Electrical conductivity of samples was calculated from the thermal conductivity by using Wiedmann-Franz Equation as follows [21, 22].

$$\frac{\lambda}{\sigma T} = L = 2.443 \times 10^{-8} \left(\frac{W.\Omega}{K^2} \right) \dots \dots \dots (7)$$

λ = thermal conductivity (W/(K.m))

σ = electric conductivity ($\Omega^{-1} . m^{-1}$)

T = absolute temperature (K)

L = lounrse number = $2.443 \times 10^{-8} \left(\frac{W.\Omega}{K^2} \right)$

XRD Test

X-ray diffraction device (type: SHIMADZU, made in Japan) utilizing copper target was used to observe the formed phases which was identified by comparing the obtained inter-atomic distance values with a standard tables according to ASTM by using analytic program match! 3.

Results and Discussion

Effect of Reinforcement Materials on Relative Density and True Porosity

Figure (5) exhibits the relationship between relative density and reinforcement material (yttria and tin). It can be observed that increasing Y₂O₃ content in Cu-Y₂O₃ composite decreases relative density, where it is reduced from 94% to 86% with 0 and 10 wt.% Y₂O₃ respectively. This is due to the increased porosity content with increasing Y₂O₃ as shown in figure (6). The porosity increase is attributed to the lack of wettability between ceramic materials and copper[23], agglomeration of yttria particles, and to the particles size of both Cu and Y₂O₃ which is near to each other, which prevent Y₂O₃ to act as filler in copper matrix.

On adding Y₂O₃ to (95%Cu – 5%Gr) matrix, relative density increases to reach (86%) with 4 wt.%Y₂O₃. This desirable effect is attributed to the high initial porosity of (95%Cu- 5%Gr) composite, which reaches 18% since Y₂O₃ acted as filler in that composite. This effect is enhanced by graphite particles, which help small Y₂O₃ particles to slip toward pore sites. Increasing Y₂O₃ beyond 4 wt.% reduces relative density through the decrease of filling action of Y₂O₃, agglomeration tendency of Y₂O₃ particles and the accompanied increase in porosity, and finally to the insulation effect of both graphite and yttria which reduces consolidation and densification of copper matrix. From the above results, it is found that 4 wt.%Y₂O₃ is the most suitable addition to (95%Cu- 5%Gr) from relative density view point.

In Figure (5), it is also observed that increasing tin content in both Cu-Sn

composites and ((95%Cu-5%Gr)-4%Y₂O₃)-Sn composites increase relative density while true porosity decreases on increasing tin content as shown in Figure (6). On sintering at 900 °C, tin melts and liquid sintering mechanism will be activated. Activation of liquid sintering mechanism enhances filling process of porosity, consolidation and densification of composites. Referring to Figures (5) and (6) it is observed that Cu-Sn composites have higher density and lower porosity than Cu-Gr-Y₂O₃-Sn composites due to the inherent porosity that accompanies graphite and yttria presence in these composites. However, on increasing tin content the density of both plain Sn-Cu and hybrid Cu- composites becomes near to each other. The same is true for true porosity. This behavior is attributed to the increased activity of tin in porosity filling and densification action with increasing its content.

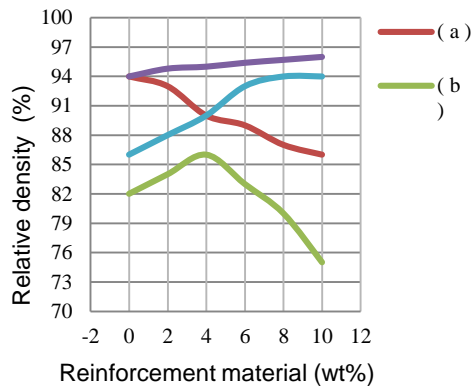


Fig.5. Relationship between relative density and reinforcement materials [(a) Cu-Y₂O₃ (b) Y₂O₃ + (95%Cu-5%Gr) (c) Cu-Sn (d) Sn + ((95%Cu-5%Gr)-4% Y₂O₃)]

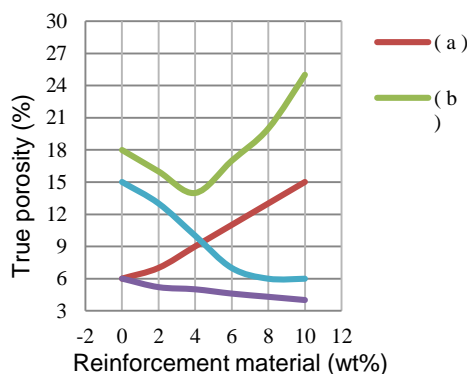


Fig. 6. Relationship between true porosity and reinforcement materials [(a)Y₂O₃ (b)Cu-Y₂O₃+(95%Cu-5%Gr) (c)Cu-Sn (d)Sn+((95%Cu-5%Gr)-4% Y₂O₃)]

Effect of Reinforcement Materials on Thermal and Electrical Conductivity

Figures (7) and (8) show that increasing Y₂O₃ content reduces both thermal and electrical conductivity of Cu-Y₂O₃ composites, where thermal conductivity reduces from 272.837 W/(m.K) to 126.5023 W/(m.K) and electrical conductivity reduces from (38.1164) (μΩ.m)⁻¹ to (17.6728) (μΩ.m)⁻¹ by increasing yttria content from 0 wt.% to 10 wt.% respectively. This behavior can be attributed to the continuous increase in porosity with increasing yttria content and to the lower thermal and electrical conductivity of yttria are (13 W/(K.m) and 0.04 (μΩ.m)⁻¹respectively). Similar behavior was previously obtained for Cu-Y₂O₃ microcomposites [24].

On the other hand, addition of Y₂O₃ to (95%Cu-5%Gr)composite results in an increase in thermal and electrical conductivity up to 4% Y₂O₃ where these conductivities were increased from (159.1549)W/(m.K) to (179.1504) W/(m.K) and from (22.2345) μΩ⁻¹.m⁻¹ to (25.111) μΩ⁻¹.m⁻¹ respectively by increasing yttria content from 0 wt.% to 4wt.% respectively. Any addition of yttria after 4wt.% results in continuous reduction in both thermal and electrical conductivities. This behavior represents a direct reflection of true porosity behavior of these composites as shown in figure (6).

Figures (7) and (8) reveal that Cu-Y₂O₃ composites have always higher thermal and electrical conductivity than (95%Cu-5% Gr)-Y₂O₃ composites. This is due to the higher porosity level for (95%Cu-5%Gr)-Y₂O₃ composites which acts as insulation sites.

Figure (7) and (8) also reveal the effect of tin content on thermal and electrical conductivity of Cu- Sn and hybrid Cu- Gr-Y₂O₃- Sn composites. It is observed that Sn reduces both thermal and electrical conductivity of Cu- Sn composites where thermal conductivity reduces from 272.8370 W/(m.k) to 165.8701 W/(m.k) and electrical conductivity from 38.1164 (μΩ.m⁻¹) to 23.1727 (μΩ.m)⁻¹ at 0wt.% and 10wt% tin respectively. This is due to the lower thermal and electrical conductivity of tin itself and to the Cu₆Sn₅ intermetallic compound that is formed on sintering as is shown in XRD patterns that will be discussed later. Thermal and electrical conductivity of Sn and Cu₆Sn₅ are 227W/(K.m), 21.7 (μΩ. m)⁻¹[20] and

39W/(K.m)[25], $5.7(\mu\Omega.m)^{-1}$ [26,27] respectively. While thermal and electrical conductivity of copper are 397 W/(K.m) and $60(\mu\Omega.m)^{-1}$ respectively[20].

On adding tin to hybrid composites, thermal and electrical conductivity firstly increases till 4wt.%Sn; where thermal and electrical conductivity increase from 169.1504 W/(K.m) to 185.2463 W/(K.m) and from $23.6309(\mu\Omega.m)^{-1}$ to $25.8796(\mu\Omega.m)^{-1}$ at 0wt.% and 4wt.% respectively. This increase is attributed to reduction in porosity by filling action of tin. After this percentage both thermal and electrical conductivity reduce to 120.230 W/(m.k) and $16.797\mu\Omega^{-1}.m^{-1}$ respectively at 10%Sn due to reduction in area fraction of copper matrix.

Figure (7) and (8) also show that both thermal and electrical conductivity of hybrid Cu-Gr- Y_2O_3 -Sn composites is always lower than Cu-Sn composites. This is due to the presence of low thermal and electrical conductivity constituents i.e. graphite, and yttria besides tin where their presence is on the account of the reduction in copper matrix with its higher thermal and electrical conductivity.

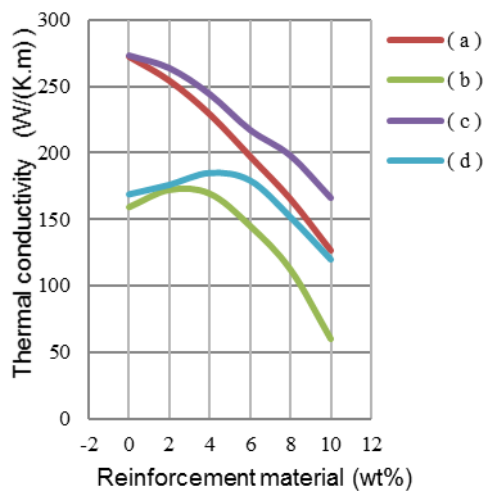


Fig. 7. Relationship between thermal conductivity and reinforcement materials [(a) Cu- Y_2O_3 (b) $Y_2O_3 + (95\%Cu-5\%Gr)$ (c) Cu-Sn (d) Sn+((95%Cu-5%Gr)-4% Y_2O_3)]

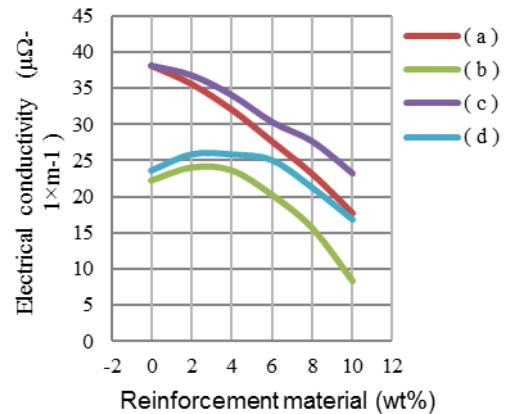


Fig. 8. Relationship between electrical conductivity and reinforcement materials [(a) Cu- Y_2O_3 (b) $Y_2O_3 + (95\%Cu-5\%Gr)$ (c) Cu-Sn (d) Sn+((95%Cu-5%Gr)-4% Y_2O_3)]

Effect of Reinforcement Materials on Hardness

Figure (9) shows the effect of Y_2O_3 addition on Brinell hardness of Cu- Y_2O_3 and (95 wt.% Cu-5 wt.%Gr) – Y_2O_3 composites. This figure illustrates that increasing yttria content increases the hardness of both composites where Brinell hardness increases from (62.3)HB to (76.2)HB and from (56.4)HB to (67.5)HB by increasing Y_2O_3 content from 0 to 10wt.% of Cu- Y_2O_3 and (95wt.%Cu-5 wt.%Gr) – Y_2O_3 composites respectively. Y_2O_3 increases composite hardness firstly by the hard nature of its particles and their action in hindering the dislocation motion and secondly by their effect as grain growth inhibitor. Furthermore, the great difference in thermal expansion between yttria reinforcement and copper matrix promotes dislocations to be produced and their density to be increased at the interface between reinforcement and matrix. This increase in dislocation density contributes in increasing the composite hardness[28, 29]. It can also be observed from Figure (9) that Cu- Y_2O_3 composites are always harder than (95wt.%Cu-5wt.%Gr)- Y_2O_3 composites. This behavior is attributed to the higher porosity level in (95wt.%Cu-5wt.%Gr)- Y_2O_3 composites as shown in figure (6) and to the contribution of graphite particles in reducing composite hardness.

Figure (9) also shows the relationship between tin and the hardness of both copper-tin composites and hybrid copper-graphite-yttria composites. The hardness of

both types of composites increases with increasing tin content up to 6wt.% while any further addition of tin beyond 6wt.% reduces Brinell hardness of both composites. For Cu-Sn composites hardness was found to be (62.3, 64.88, and 58.33) HB at (0, 6 and 10)wt.%Sn respectively. While for Cu-Gr-Y₂O₃-Sn composites, it was found to be (58.3, 69.15, and 61.37) HB at (0, 6, 10)wt.%Sn respectively. Tin addition increases Brinell hardness through reducing porosity, enhanced consolidation and densification by liquid sintering mechanism and partly through the formation of the hard intermetallic compound Cu₆Sn₅ [30] besides solid solution hardening. However on increasing tin content above 6wt.% composites hardness decreases due to the soft nature of tin and to the excess formation of Cu₆Sn₅ which precipitates at Cu-Sn interface leading to weak bond between copper matrix and tin reinforcement particles.

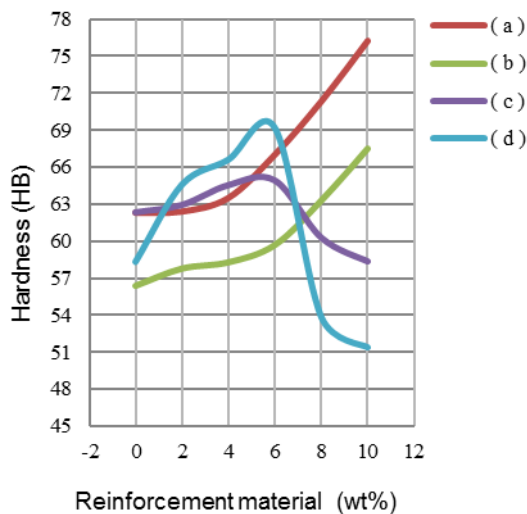


Fig. 9. Relationship between the hardness and reinforcement materials [(a) Cu-Y₂O₃ (b) Y₂O₃ + (95%Cu-5%Gr) (c) Cu-Sn (d) Sn + ((95%Cu-5%Gr)- 4% Y₂O₃)]

Effect of Reinforcement Materials on Wear Rate

Figure (10) reveals that increasing yttria content in Cu-Y₂O₃ Y₂O₃ content as shown in Figure (9). However increasing Y₂O₃ content beyond 6wt.% leads to the formation of yttria agglomerates which weaken the bond between yttria and the

matrix as well as increasing of the porosity. These agglomerates have harmful effects on the bonding between reinforcement and matrix besides their harmful effects on the nature of the interface where microporosity prefers to form at these sites [24, 31]. Addition of yttria to 95wt%Cu-5wt%Gr composite reduces wear rate till 4%Y₂O₃ where wear rate reaches (0.56×10⁻⁷) g/cm. Increasing yttria content over 4wt% increases wear rate continuously to reach (1×10⁻⁷)g/cm at 10wt%.

Figure (10) also reveals that (95%Cu-5%Gr)-Y₂O₃ composites have always lower wear rate than plain Cu-Y₂O₃ composites. This is due to the combined effects of graphite which reduces wear rate through its lubrication effect and yttria particles through their higher hardness. (95%Cu-5%Gr)-Y₂O₃ composites is found to give the lowest wear rate among all other composites with some reduction in thermal and electrical conductivity, so it is selected as basic composition for the addition of tin as an additional constituent.

In Figure (10), it is observed that wear rate of both copper-tin composite and hybrid copper composites reduces with increasing tin contents till 6 wt% tin, where it decreases from (1.7×10⁻⁷)g/cm to (0.7×10⁻⁷)g/cm and from (0.57 ×10⁻⁷)g/cm to (0.18×10⁻⁷)g/cm for both composites respectively. This is attributed to the same factors that increase Brinell hardness of these composites. Increasing tin content above 6wt.% increases wear rate remarkably for both types of composites. This is attributed mainly to precipitation of the brittle Cu₆Sn₅ intermetallic compound at Cu-Sn interfaces, which weakens them leading to dislocation or fragmentation of these particles from rubbed surface easily under the effect of friction forces and increases wear rate of these composites.

Throughout the present study, it is found that hybrid copper composite with 5wt%Gr-4wt%Y₂O₃-6wt%Sn is considered to be the best among all other composites where it shows the lowest wear rate and good thermal and electrical conductivity.

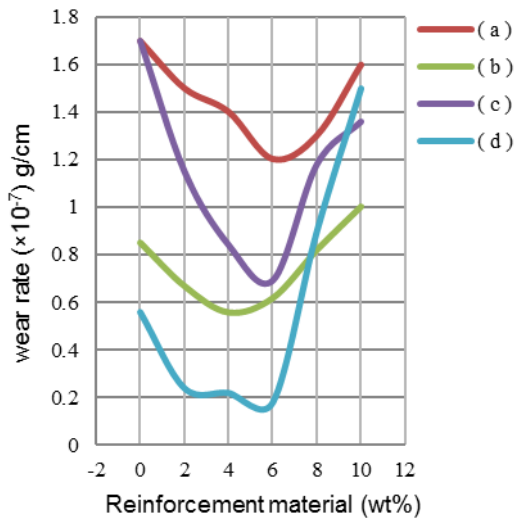


Fig. 10. Relationship between the wear rate and reinforcement materials [(a)Cu-Y₂O₃ (b) Y₂O₃ + (95%Cu-5%Gr) (c) Cu-Sn (d) Sn + ((95%Cu-5%Gr)- 4% Y₂O₃)]

X-Ray Diffraction (XRD) Test

Figure (11) shows the XRD pattern of pure copper compact. All the prominent peaks (high intensity) belong to metallic copper. No any sign of oxidation.

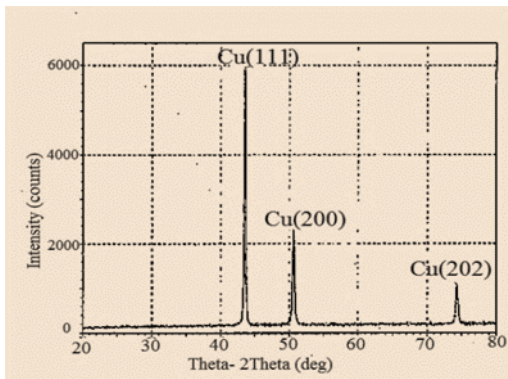


Fig. 11. XRD pattern of pure copper compacts

Figure (12) shows the XRD pattern of Cu-5wt.%Gr composite. It is observed that the strong peaks belongs to metallic copper and relatively weak peak (low intensity) belongs to graphite. Not any reaction between copper matrix and graphite reinforcement was taking place on sintering.

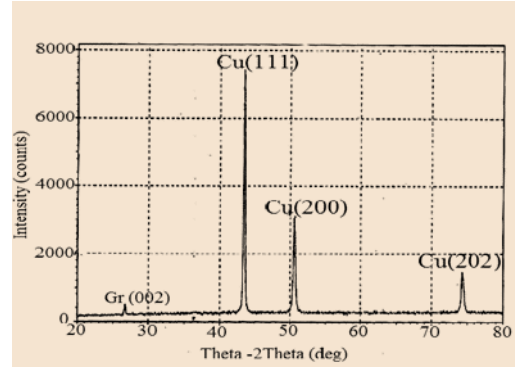


Fig. 12. XRD pattern of Cu-5%Gr composite

Figures (13) and (14) show XRD patterns of Cu-6wt.%Y₂O₃ and Cu-10wt.%Y₂O₃ composites respectively. It is observed that the presence of the intermetallic Cu₂Y₂O₅ compound due to occurrence of partial reaction between yttria and copper. Peaks of copper are also the prominent peaks in these composites. Absence of copper oxide peaks confirms that no oxidation takes place during sintering.

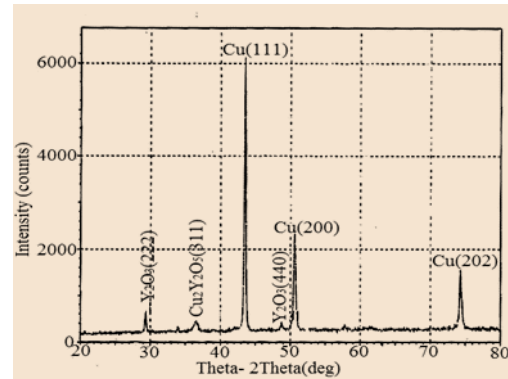


Fig. 13. XRD pattern of Cu-6%Y₂O₃ composite

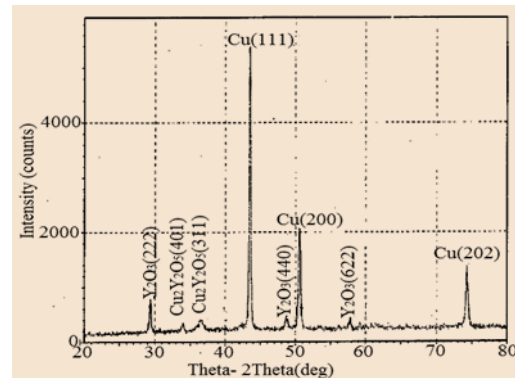


Fig. 14. XRD pattern of Cu-10%Y₂O₃ composite

Figures (15) and (16) show XRD for (95%Cu-5%Gr)-4%Y₂O₃ and (95%Cu-5%Gr)-10%Y₂O₃ composites respectively. Clear major peaks of Cu, Gr, Y₂O₃ and Cu₂Y₂O₅ are observed in these composites. Increasing yttria content increases intensity of yttria and Cu₂Y₂O₅ peaks.

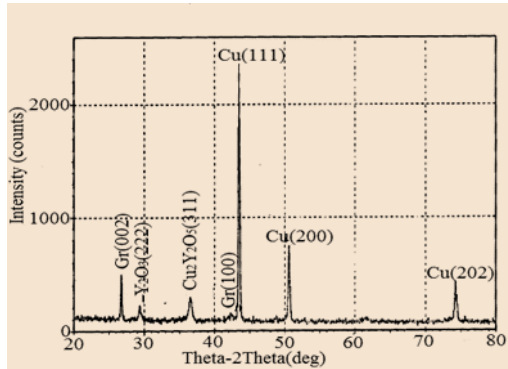


Fig. 15. XRD pattern of Cu-5%Gr-4%Y₂O₃ composite

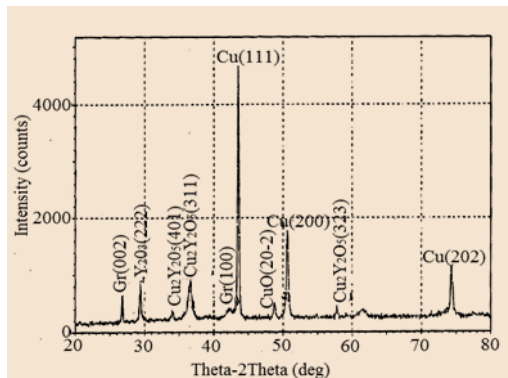


Fig. 16. XRD pattern of Cu-5%Gr-10%Y₂O₃ composite

Figures (17), (18) and (19) represent the XRD patterns of Cu-4%Sn, Cu-6%Sn and Cu-10%Sn composites respectively. Strong peaks of Cu₆Sn₅ was observed in all composites. Peak intensity increases with increasing Sn content. No sign of metallic Sn was observed. This is due to the complete reaction between copper and tin on sintering.

Figure (20) shows the XRD pattern of the hybrid (95wt%-5wt%)-10wt%Y₂O₃-6wt%Sn composite. Major peaks were found to belong to metallic Cu, Gr, Y₂O₃, Sn, Cu₂Y₂O₅ and Cu₆Sn₅. Moreover, peak intensity of Cu was found in this composite is lower than these present in other composites due to the presence of high amounts of other constituents and the

reaction between some of these constituents and copper.

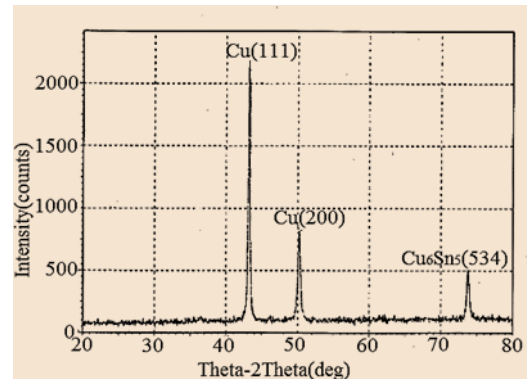


Fig. 17. XRD pattern of Cu-4%Sn composite

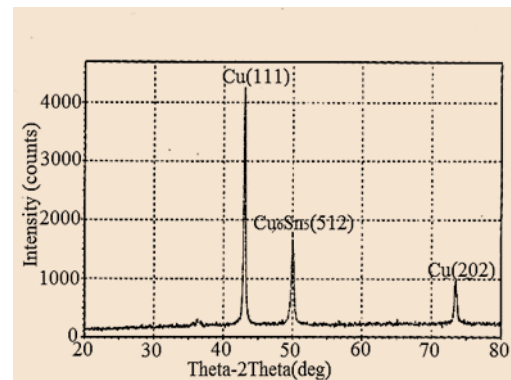


Fig. 18. XRD pattern of Cu-6%Sn composite

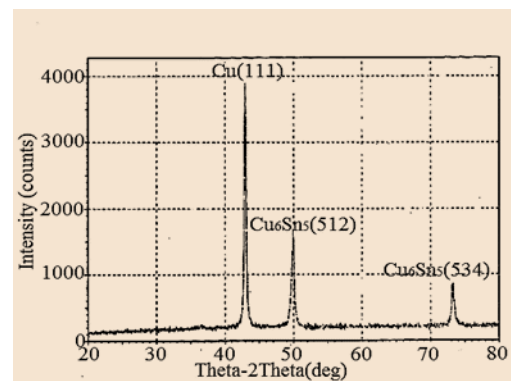


Fig. 19. XRD pattern of Cu-10%Sn composite

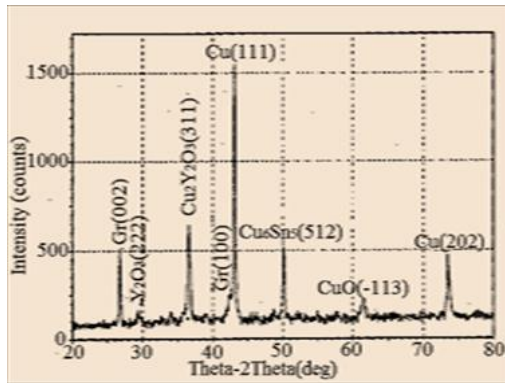


Fig. 20. XRD pattern of ((95%Cu-5%Gr)-10%Y₂O₃)-6%Sn composite

Conclusions

- 1- Hybrid Copper-graphite composites have been successfully prepared by powder metallurgy technique.
- 2- (95wt.%Cu-5wt.%Gr)-Y₂O₃ composites have always lower wear rate than plain Cu-Y₂O₃ composites.
- 3- Hardness and true porosity of the composites increases with increasing yttria content.
- 4- Thermal and electrical conductivity of the composites decreases with increasing yttria content.
- 5- Thermal and electrical conductivity of Cu-Gr-Y₂O₃-Sn composites is always lower than those of Cu-Sn composites.
- 6- Addition of tin to both pure copper and (95%Cu-5%Gr)-4%Y₂O₃ composites reduces true porosity.
- 7- Increasing tin content up to 6wt.% increases the composite hardness despite the the matrix composition.
- 8- Thermal and electrical conductivity of Cu-Sn composites reduce with increasing of tin content.
- 9- Thermal and electrical conductivity of hybrid ((95%Cu-5%Gr)-4%Y₂O₃-Sn composite increases with increasing tin content till 4%Sn.
- 10- The best composite which found in this work is ((95% Cu-5% Gr)-4% Y₂O₃)-6% Sn which has true porosity 7%, relative density 93%, hardness (69.15 HB), wear rate (0.18×10⁻⁷ g/cm), thermal conductivity 179.507 W/k.m) and electrical conductivity (25.0778 μΩ⁻¹.m⁻¹).

References

1. Molina A, Torres-Islas A, Serna S, Acosta-Flores M, Rodriguez-Diaz RA, Colin J. Corrosion, electrical and mechanical performance of copper

matrix composites produced by mechanical alloying and consolidation. *International Journal of Electrochemical Science* 2015;10: 1728-1741.

2. ASM Handbook Volume 21: Composites, Editor: D.B. Miracle and S.L. Donaldson, 2001.
3. Firkowska I, Boden A, Boerner B, Reich S. The origin of high thermal conductivity and ultralow thermal expansion in copper-graphite composites. *Nano Letters, American Chemical Society* 2015;15:4745–4751.
4. Joshi PB, Rehani BK, Palak PS, Khanna PK. Studies on copper-Yttria nano-composites: high-energy ball milling versus chemical reduction method. *Journal of Nanoscience and Nano-technology* 2012;12(3):2591-2597.
5. Long BD, Othman R, Zuhailawati H, Umemoto M.2014. Comparison of two powder processing techniques on the properties of Cu-NbC composites. *Journal of Advances in Materials Science and Engineering* 2014:1-6.
6. Shabania MM, Paydara MH, Zamirib R, Goodarzi M, Moshksara MM. Microstructural and sliding wear behavior of Sic-particle reinforced copper matrix composites fabricated by sintering and sinter-forging processes. *Journal of Materials Research and Technology* 2016;5(1): 5–12.
7. Leemaa N, Radhab P, Vettivelc SC, Nehemiah HK. Characterization, pore size measurement and wear model of a sintered Cu-W nano composite using radial basis functional neural network. *Materials and Design* 2015;68:195–206.
8. Chyad FA, Agoal IR, Mutter MM. Effect of addition Sic particles on the hardness and dry sliding wear of the copper-graphite composite. *The Iraqi Journal for Mechanical and Material Engineering* 2012;12(2):298-304.
9. Amrishraj D, Senthilvelan T. Modelling and optimization of sliding wear behaviour of copper- graphite composites. In: *Proceedings of Second International Conference on Advances in Industrial Engineering Applications* 2014 Jan 6-8; Chennai. Anna University: p. 116-123.

10. Gu D, Shen Y. Effects of dispersion technique and component ratio on densification and microstructure of multi-component Cu-based metal powder in direct laser sintering. *Journal of Materials Processing Technology* 2007;182(1-3):564–573.
11. Dewidar M, Abdel-Jaber GT, Bakrey M, Badry H. 2010. Effect of processing parameters and amount of additives on the mechanical properties and wear resistance of copper-based composite. *International Journal of Mechanical & Mechatronics Engineering* 2010;10(3): 25-40.
12. Jin Y, Hu M. Densification of graphite/copper compound powders. *IEEE* 2011:1131-1135.
13. Samal CP. Microstructure and mechanical property study of Cu-graphite metal matrix composite prepared by powder metallurgy route. M.T Project Thesis. Orissa, India: National Institute of Technology Rourkela Odisha;2012.
14. Prapai J, Morakotjinda M, Yotkaew T, Vetayanukul B, Tongsi R, Kamsuwan P, Yoshino P, Tribological properties of PM Cu-based dry friction clutch. *Key Engineering Materials* 2013;545:163-170.
15. Mahdi FM, Razooqi RN, Irhayyim SS. Effect of graphite content and milling time on physical properties of copper-graphite composites prepared by powder metallurgy route. *Australian Journal of Basic and Applied Sciences* 2013;7:245-255.
16. Chawla N, Chawla KK. *Metal Matrix Composites*. 1st ed., USA: Springer Publisher; 2006.
17. ASTM C373 – 88. Standard test method for water absorption, bulk density, apparent porosity, and apparent specific gravity of fired white ware products. *American Society for Testing and Materials* 2006; Philadelphia, Reapproved.
18. Dutta G, Bose D. Effect of sintering temperature on density, porosity and hardness of a powder metallurgy component. *International Journal of Emerging Technology and Advanced Engineering* 2012;2(8):121-123.
19. Jain S, Rana RS, Jain P. Study of microstructure and mechanical properties of Al-Cu metal matrix reinforced with B₄C particles Composite. *International Research Journal of Engineering and Technology* 2016;3(1):499-504.
20. William D. Jr C. *Fundamentals of materials science and engineering*. 5th ed., USA; 2001.
21. Hamid ZA, Moustafa SF, Morsy FA, Atty Khalifa NA, Abdel Mouez F. Fabrication and characterization copper/diamond composites for heat sink application using powder metallurgy. *Natural Science* 2011;3: 936-947.
22. Kováčik J, Affiliated SE, Bielek J. Cross-property connections for copper-graphite composites. *Acta Mechanica* 2016;227:105-112.
23. Barzilai S, Aizenshtein M, Froumin N, Frage N. Y₂O₃/(Cu-Me) systems (Me=Al, Ti): Interface reactions and wetting. *Journal of Materials Science* 2012;41(16):5108-5112.
24. Stobrawa JP, Rdzawski ZM, Głuchowski WJ. Microstructure and properties of nanocrystalline copper-yttria microcomposites. *Journal of Achievements in Material and Manufacturing Engineering* 2007;24(2):83-86.
25. Miyake S, Nagano Y, Miyake Y, Takamatsu H, Kita T. Spatially resolved thermal conductivity of intermetallic compounds measured by micro-thermo-reflectance method. *Journal of Japan Institutes of Metals* 2010;74(11):740-745.
26. Podzemsky J, Papez V, Urbanek J, Dusek K. influence of intermetallic compounds on RF resistance of joints soldered with lead free alloys. *Radioengineering* 2012;21(2):573-579.
27. Jones J. *Tin whiskers and copper/tin intermetallics*. UK: Alter Technology Group 1000 Lakeside, North Harbour, Portsmouth Hampshire;2006.
28. Simchia H, Simchia A. Tensile and fatigue fracture of nanometric alumina reinforced copper with bimodal grain size distribution. *Journal of Materials Science and Engineering: A* 2009;507(1-2):200–206.
29. Casati R, Vedani M. Metal matrix composites reinforced by nanoparticles—A review. *Metals - Open Access Metallurgy Journal* 2014;4(1):65-83.
30. Fields JRJ, Low SR, Lucey GK. Physical and mechanical properties of intermetallic compounds commonly found in solder joints. Published

- in Metal Science of Joining, Proceedings of TMS Symposium, Cincinnati, Oct 20-24, 1991.
31. Chandrakanth RG, Rajkumar K, Aravindan S. Fabrication of copper–
tic–graphite hybrid metal matrix composites through microwave processing. International Journal of Advanced Manufacturing Technology 2010;48(5-8):645–654.